



Porous Nanocrystalline Silicon Supported Bimetallic Pd-Au Catalysts: Preparation, Characterization, and Direct Hydrogen Peroxide Synthesis

Dmitriy I. Potemkin^{1,2*}, Dmitry K. Maslov², Konstantin Lopotnov³, Pavel V. Snytnikov^{1,2}, Yuri V. Shubin^{1,4}, Pavel E. Plyusnin^{1,4}, Dmitry A. Svintsitskiy^{1,2}, Vladimir A. Sobyanyin² and Alexei A. Lapkin^{3,5*}

OPEN ACCESS

Edited by:

Heqing Jiang,
Qingdao Institute of Bioenergy and
Bioprocess Technology (CAS), China

Reviewed by:

Yan Zhang,
Qingdao Institute of Bioenergy and
Bioprocess Technology (CAS), China
Mingxing Wu,
Hebei Normal University, China

*Correspondence:

Dmitriy I. Potemkin
potema@catalysis.ru
Alexei A. Lapkin
aal35@cam.ac.uk

Specialty section:

This article was submitted to
Chemical Engineering,
a section of the journal
Frontiers in Chemistry

Received: 30 January 2018

Accepted: 12 March 2018

Published: 27 March 2018

Citation:

Potemkin DI, Maslov DK, Lopotnov K,
Snytnikov PV, Shubin YV, Plyusnin PE,
Svintsitskiy DA, Sobyanyin VA and
Lapkin AA (2018) Porous
Nanocrystalline Silicon Supported
Bimetallic Pd-Au Catalysts:
Preparation, Characterization, and
Direct Hydrogen Peroxide Synthesis.
Front. Chem. 6:85.
doi: 10.3389/fchem.2018.00085

¹ Laboratory of the Energy-Efficient Catalytic Processes, Novosibirsk State University, Novosibirsk, Russia, ² Department of Heterogeneous Catalysis, Boreskov Institute of Catalysis, Novosibirsk, Russia, ³ Department of Chemical Engineering and Biotechnology, University of Cambridge, Cambridge, United Kingdom, ⁴ Laboratory of the Rare Platinum Metals Chemistry, Nikolaev Institute of Inorganic Chemistry, Novosibirsk, Russia, ⁵ Cambridge Centre for Advanced Research and Education in Singapore Ltd., Singapore, Singapore

Bimetallic Pd-Au catalysts were prepared on the porous nanocrystalline silicon (PSi) for the first time. The catalysts were tested in the reaction of direct hydrogen peroxide synthesis and characterized by standard structural and chemical techniques. It was shown that the Pd-Au/PSi catalyst prepared from conventional H₂[PdCl₄] and H[AuCl₄] precursors contains monometallic Pd and a range of different Pd-Au alloy nanoparticles over the oxidized PSi surface. The PdAu₂/PSi catalyst prepared from the [Pd(NH₃)₄][AuCl₄]₂ double complex salt (DCS) single-source precursor predominantly contains bimetallic Pd-Au alloy nanoparticles. For both catalysts the surface of bimetallic nanoparticles is Pd-enriched and contains palladium in Pd⁰ and Pd²⁺ states. Among the catalysts studied, the PdAu₂/PSi catalyst was the most active and selective in the direct H₂O₂ synthesis with H₂O₂ productivity of 0.5 mol g_{Pd}⁻¹ h⁻¹ at selectivity of 50% and H₂O₂ concentration of 0.023 M in 0.03 M H₂SO₄-methanol solution after 5 h on stream at -10°C and atmospheric pressure. This performance is due to high activity in the H₂O₂ synthesis reaction and low activities in the undesirable H₂O₂ decomposition and hydrogenation reactions. Good performance of the PdAu₂/PSi catalyst was associated with the major part of Pd in the catalyst being in the form of the bimetallic Pd-Au nanoparticles. Porous silicon was concluded to be a promising catalytic support for direct hydrogen peroxide synthesis due to its inertness with respect to undesirable side reactions, high thermal stability, and conductivity, possibility of safe operation at high temperatures and pressures and a well-established manufacturing process.

Keywords: direct H₂O₂ synthesis, direct hydrogen peroxide synthesis, porous silicon, bimetallic nanoparticles, alloy nanoparticles, Pd-Au catalysts, gold-palladium catalysts, double complex salts

INTRODUCTION

In the general field of industrial chemistry the role of heterogeneous catalysis is difficult to overestimate: the advances in large-scale catalytic processes, such as ammonia synthesis, sulphuric acid and nitric acid processes, ethylene and propylene production, acetic acid, and methanol syntheses and several others were responsible for the rapid development of human civilization in the twentieth-century. In the twenty-first century the challenges for catalysis are different but, arguably, even harder than those that were solved till now: selective activation of C-H bonds in saturated alkanes, efficient and selective activation of CO₂, efficient splitting of water, highly selective functionalization of complex molecules for pharmaceutical and speciality chemicals, etc. These challenges have one common aspect—the requirement for much better control of reaction selectivity in the traditionally “difficult” reactions, such as sp³ C-H activation, as an example. The requirement for better selectivity control marks the need for a very different approach to catalysts design to that traditionally practiced in the twentieth-century for bulk processes: highly dispersed and uniform active sites are preferred (Flytzani-Stephanopoulos and Gates, 2012) and often polyfunctionality is required (Climent et al., 2014). Many conventional heterogeneous catalysts are highly *heterogeneous* in the nature of their active sites. For this reason, a significant effort in current research in the field of heterogeneous catalysis is on developing new methods of synthesis of heterogeneous catalysts, that result in much tighter control of the structure and composition of the active sites. Advanced synthesis techniques are under development: from modified impregnation and adsorption (Munnik et al., 2015) to a novel approach of nanoparticles biosynthesis which presents an alternative eco-friendly and potentially precise way for synthesis of heterogeneous catalysts (Hulkoti and Taranath, 2014).

Novel support materials do not frequently appear in catalytic literature and most conventionally-used supports, such as mixed oxides or carbon, are not well-suited to the challenge of precise control of selectivity due to their inherent heterogeneity. For this reason, significant attention is currently paid to “structured” supports, such as MOFs (Dhakshinamoorthy et al., 2013; Zhao et al., 2016), 2D materials such as graphene (Fan et al., 2015; Julkapli and Bagheri, 2015), 1D materials such as carbon nanotubes (Serp and Castillejos, 2010; Yan et al., 2015) or titanate nanotubes (Bavykin et al., 2005), and so on. Among the many support materials usually investigated in catalysis *silicon* is one of less known and little studied to date.

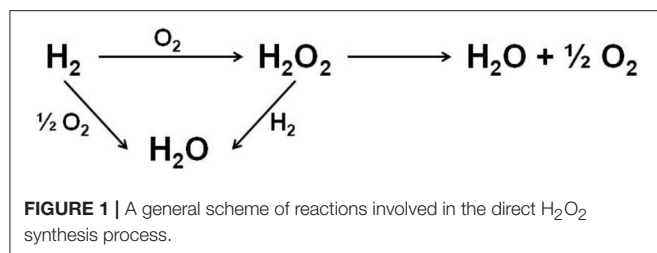
Its application as a catalyst support was first discussed in Polisski et al. (2010). PSi is a high surface area semiconducting material with high heat conductivity and pore structure very interesting for catalysis—a network of open pores with pore sizes in the mesopore range of 2–6 nm (Künzner et al., 2003); the electrochemical pore formation in silicon having been studied in detailed earlier (Lehmann et al., 2000). The high surface area of porous silicon (PSi) is hydrogen-terminated. This hydrogen can facilitate reduction of dissolved metal salts directly at the surface, without the use of additional reducing agents (Polisski

et al., 2008). This can be exploited to produce small dispersed metal nanoparticles inside PSi pores from alcoholic metal salt solutions. This synthesis method resulted in metal nanoparticles in the range of 5–10 nm, located largely within the pores of the support. This is distinct from the earlier reports of metal/PSi composites obtained from aqueous metal salt solutions using metal hydrides or hydrogen as reducing agents, which result in the formation of much larger metal particles (Coulthard et al., 1993, 2000; Coulthard and Sham, 1998). Similarly, the surfactant mediated method using sodium borohydride as reducing agent in aqueous-ethanol solution results in the formation of large metal nanoparticles in the range of 10–50 nm (Yashtulov et al., 2011, 2016).

In recent years there is a significant increase in the number of publications devoted to different synthesis methods and application fields of metal-PSi materials. To cite only few studies, porous silicon was used to synthesize nano-composite materials for lithium-ion batteries (Zhai et al., 2017), as a stoichiometric reducing agent for direct conversion of CO₂ to methanol (Dasog et al., 2017), as a support for Pd nanoparticles in catalytic oxidation of formic acid (Yashtulov and Flid, 2013), in a detailed experimental and theoretical investigation of the electronic structure and gas adsorption on Pd, Cu, Pd-Cu, and WO₃-Pd nanoparticles supported on porous silicon for gas sensing applications (Litovchenko et al., 2017), for developing Pt-Pd/PSi electrocatalysts for direct methanol fuel cell (Ensafi et al., 2015). There are no new works on developing heterogeneous catalysts for chemical processes. Thus, in order to expand current knowledge on catalysis by porous silicon-supported catalysts we chose a difficult and very important industrial chemistry reaction of direct synthesis of hydrogen peroxide.

Hydrogen peroxide is an excellent oxidizing reagent for the production of both fine and bulk chemicals that finds applications also in the area of wastewater treatment, paper and pulp bleaching, and widely used in healthcare. Most of the world's hydrogen peroxide is currently produced by the sequential hydrogenation and oxidation of an alkyl anthraquinone (Bernardotto et al., 2009). This process suffers from several limitations, such as significant amount of organic waste, need of several energy consuming separation and concentration steps and economic feasibility only in large-scale (Menegazzo et al., 2015).

The direct synthesis of H₂O₂ from hydrogen and oxygen in methanol or water reaction media provides a more atom efficient route to the current commercial production process. The direct route would enable H₂O₂ production to take place at its point of use, reducing the transportation costs, and for this reason there is a significant interest in developing such a catalytic process. The minimal required H₂O₂ concentration produced by the direct synthesis for practical use is estimated to be 1 wt.% or 0.23 M in methanol solution (Garcia-Serna et al., 2014). **Figure 1** represents reactions involved in the direct H₂O₂ production process (Bernardotto et al., 2009). Besides the target H₂O₂ synthesis reaction, undesirable total H₂ oxidation together with H₂O₂ hydrogenation and decomposition reactions could occur. Thus, catalyst's ability to synthesize H₂O₂ selectively and avoid its hydrogenation and decomposition becomes the key



factor to reach high H₂O₂ concentrations with acceptable atomic and economic efficiencies.

Several reviews (Samanta, 2008; Dittmeyer et al., 2015; Edwards et al., 2015; Yi et al., 2016; Seo et al., 2017) consider catalytic systems, reaction conditions, and engineering concepts for direct H₂O₂ synthesis. Several bimetallic Pd-based systems show promising levels of performance in the direct H₂O₂ synthesis: Pd-Au (Edwards et al., 2005, 2009), Pd-Pt (Bernardotto et al., 2009), Pd-Ni (Maity and Eswaramoorthy, 2016), novel Pd-Te (Tian et al., 2017), and Pd-Ag (Gu et al., 2016) and the recently published Pd-Sn (Freakley et al., 2016), exhibiting a very high level of performance. Among other systems the Pd-Au one exhibiting selectivities up to 95% (Edwards et al., 2009) is the most extensively studied. Earlier studies have shown that bimetallic alloy Pd-Au nanoparticles, probably with Pd-enriched shell (Edwards et al., 2005), are responsible for high activity and selectivity in H₂O₂ synthesis. The surface ratio of Pd⁰/Pd²⁺ in the AuPd alloy was found to be an important factor controlling the overall catalyst performance. A stable non-leaching form of Pd²⁺ was identified as a key feature in highly selective PdAu catalysts (Edwards et al., 2012). Catalyst surface and/or reaction media acidity play important role in the reaction. Highly acidic cesium salts of Keggin-type tungstophosphoric acid (Cs_xH_{3-x}PW₁₂O₄₀) were proposed as the best support materials, providing better performance than carbon and metal oxides supports (Ntainjua et al., 2012). A reversible high-pressure CO₂-derived acidification of combined water-methanol reaction media (Freakley et al., 2013) was successfully applied for high pressure operations. It should also be noted that in spite of huge efforts to determine the surface structure of bimetallic Pd-Au catalysts active for the H₂O₂ direct synthesis, the detailed understanding of the active sites of the metal nanoparticles remains elusive.

The selective formation of bimetallic Pd-Au nanoparticles in supported catalysts is desirable to obtain highly selective direct H₂O₂ synthesis catalyst, due to ability of monometallic Pd particles to catalyze hydrogenation of H₂O₂ (Edwards et al., 2015), thereby limiting the achievable H₂O₂ maximum concentration and decreasing process selectivity. Within this context we applied the approach based on decomposition of double complex salts (DCS) inside the pores of a support material for the synthesis of the bimetallic Pd-Au direct H₂O₂ synthesis catalyst. DCSs of transition metals, coordination compounds with the common formula [M'L'_n][M''L''_m]_y, where M' and M'' are metals, L' and L'' are different ligands, have a number of advantages as single-source precursors of bimetallic catalysts:

- Complexing metals in a DCS are “mixed” on a molecular level that allows formation of alloys upon salt decomposition;
- Stoichiometry of a precursor complex determines composition of the alloys;
- Ability to preset exact phase composition and morphology of the alloy nanoparticles, varying the DCS deposition process, and decomposition conditions.

The successful application of DCS for catalyst preparation was demonstrated in a number of works (Potemkin et al., 2012, 2014, 2017; Shubin et al., 2012; Simonov et al., 2012; Bulushev et al., 2013; Vedyagin et al., 2013, 2014). To provide Pd-Au interaction and to promote alloy formation we have chosen [Pd(NH₃)₄][AuCl₄]₂ DCS as a single-source precursor. Its properties and application as a precursor for bimetallic Pd-Au nanoparticles were discussed in Shubin et al. (2012), Bulushev et al. (2013), Simonov et al. (2012), and Plyusnin et al. (2007). Due to the fact, that Pd and Au atoms are premixed in the precursor, [Pd(NH₃)₄][AuCl₄]₂ reduction inside the pore space at mild conditions leads to the selective formation of supported Pd-Au alloy nanoparticles without intermediate formation of Pd and Au phases and its alloying.

Besides the composition and structure of metallic component the choice of support plays an important role in designing direct H₂O₂ synthesis catalysts. Support's properties, such as red-ox interaction with Pd, wettability by reaction media, inertness with regard to H₂O₂ decomposition and hydrogenation, surface acidity are of special attention. Carbon supports (Edwards et al., 2009), titania (Edwards et al., 2005), Keggin-type heteropolyacids (Ntainjua et al., 2012), sulfated ceria and zirconia (Menegazzo et al., 2015) are considered as conventional choice for direct H₂O₂ synthesis catalysts. However, the search for alternative supports is still actual, especially in the scope of further reaction translation from lab-scale batch reactors to more practical and scalable continuous flow multiphase reactors, in which the application of conventional catalysts powders is limited by the need of its fixing and mass-/heat-transfer problem.

In this regard we investigated the properties of porous nanocrystalline silicon powder (PSi) as a support for Pd-Au direct H₂O₂ synthesis catalysts. We report results on preparation, characterization and catalytic tests of bimetallic PSi supported Pd-Au catalysts prepared by [Pd(NH₃)₄][AuCl₄]₂ single-source precursor decomposition. To our knowledge it is the first report of such catalytic system and extends the knowledge of porous silicon as a promising catalyst support. The comparison with monometallic PSi supported Pd and Au catalysts, and bimetallic Pd-Au catalyst, prepared utilizing conventional H₂[PdCl₄] and H[AuCl₄] precursors, were done as well.

EXPERIMENTAL

Materials

Porous nanocrystalline silicon with average grain size of 4 μm was supplied by Vesta Ceramics. All other chemicals were commercially purchased and used without additional purification.

Catalyst Preparation

All catalysts were prepared by the metals reduction from its salts solutions by PSi's surface H-terminal atoms by the protocol adapted from Polisski et al. (2010).

The Pd loading in all catalysts was set to 2 wt.% which is close to optimal value according to literature (Edwards et al., 2005).

The synthesized $[\text{Pd}(\text{NH}_3)_4][\text{AuCl}_4]_2$ DCS was used as a single-source precursor for the PdAu₂/PSi catalyst. The Pd and Au loadings were set to 2 and 7.4 wt.% according to $[\text{Pd}(\text{NH}_3)_4][\text{AuCl}_4]_2$ stoichiometry. A portion of 2 g of PSi powder was added to 50 mL of the DCS acetone solution of the required concentration at -15°C under vigorous stirring. Acetone solvent was used to attain wetting of the hydrophobic H-terminated surface of PSi and due to high $[\text{Pd}(\text{NH}_3)_4][\text{AuCl}_4]_2$ solubility in acetone. The suspension was kept at -15°C for 1 h under vigorous stirring, and then temperature was slowly increased to ambient. The obtained catalyst was filtered, washed several times with acetone and warm water to dissolve possible residual salts in pores, and dried at room temperature on air.

Bimetallic Pd-Au/PSi catalyst was prepared according to the procedure described above using the conventional $\text{H}_2[\text{PdCl}_4]$ and $\text{H}[\text{AuCl}_4]$ joint water-ethanol solution as a metal source. The Pd and Au loadings for Pd-Au/PSi catalyst were set to 2 wt.%, which are close to the optimal values according to the literature data (Edwards et al., 2009).

Monometallic Pd/PSi and Au/PSi catalysts were prepared using the same protocol with water-acetone solutions of $[\text{Pd}(\text{NH}_3)_4](\text{NO}_3)_2$ and $\text{H}[\text{AuCl}_4]$ as precursors.

Catalytic Activity Study

Catalytic tests were carried out at atmospheric pressure at -10°C in a thermostated glass reactor. Mixing was carried out with an inert rotor operating at 400 rpm. Oxygen and hydrogen were bubbled by a gas diffuser directly into the liquid phase with a total flow of 50 ml (STP) min^{-1} . A non-explosive gas mixture with the following composition was used: 4 vol.% H_2 and 96 vol.% O_2 . The reaction medium was 100 mL of a 0.03 M H_2SO_4 methanol solution. Catalyst loading of 50 mg was used. After the catalyst addition the suspension was stirred and then kept for 20 min in an ultrasonic bath. After that samples were pretreated *in situ* at room temperature first by H_2 [30 min, 30 ml (STP) min^{-1}] and then by O_2 (20 min, 30 $\text{scm}^3 \text{min}^{-1}$). Prior to starting the reaction, reactor was purged with He [50 ml (STP) min^{-1}]. During catalytic tests small aliquots of the liquid phase were sampled through a septum and used for hydrogen peroxide concentration determination.

H_2O_2 concentration was measured by iodometric titration. H_2 concentrations at the inlet and the outlet of the reactor were measured by a quadrupole MS (Stanford research). The catalyst's performance was characterized in terms of the H_2O_2 concentration in methanol solutions ($[\text{H}_2\text{O}_2]$), H_2 conversion (X_{H_2}) and the selectivity toward H_2O_2 synthesis ($S_{\text{H}_2\text{O}_2}$), which were calculated from the following equations:

$$X_{\text{H}_2} = \frac{[\text{H}_2]_{\text{inlet}} - [\text{H}_2]_{\text{outlet}}}{[\text{H}_2]_{\text{inlet}}} \cdot 100\%,$$

$$S_{\text{H}_2\text{O}_2} = \frac{n_{\text{H}_2\text{O}_2}}{\Delta n_{\text{H}_2}} \cdot 100\%,$$

where $[\text{H}_2]_{\text{inlet}}$ and $[\text{H}_2]_{\text{outlet}}$ are the average H_2 inlet and outlet concentrations during the period between aliquots sampling; $n_{\text{H}_2\text{O}_2}$ is the amount of H_2O_2 formed during the period between aliquots sampling; Δn_{H_2} is the amount of H_2 consumed during the period between aliquots sampling.

The catalyst loading and reaction temperature were optimized in order to make hydrogen conversion insensitive to stirring speed.

Experiments on H_2O_2 decomposition and hydrogenation were carried out at the same conditions as H_2O_2 synthesis. The initial H_2O_2 concentration was set to ca. 70 mM ($70 \cdot 10^{-3} \text{ mol L}^{-1}$), gas feed composition: pure He for H_2O_2 decomposition and 4 vol.% H_2 and 96 vol.% He for H_2O_2 hydrogenation tests. The gas flow was set to 50 $\text{scm}^3 \text{min}^{-1}$. H_2O_2 concentration was measured one time per hour during 5 h.

Pure PSi support was treated by the water-acetone solution using the protocol described in section Catalyst Preparation and was tested in H_2O_2 synthesis, decomposition and hydrogenation. PSi did not show any activity in this reaction. Thus, one can conclude that PSi material is inert with regard to H_2O_2 synthesis, decomposition, and hydrogenation and could be successfully used as a catalyst support for direct synthesis of H_2O_2 .

Catalyst Characterization

The as-prepared catalysts were characterized by a number of physico-chemical techniques. The chemical composition of the catalysts was determined by inductively coupled plasma atomic emission spectrometry (an Optima instrument).

The specific BET surface area (S_{BET}) and pore volume (V_p) of the catalysts were determined from the complete nitrogen adsorption isotherms at -196°C (ASAP 2400 instrument).

XRD analysis of the as-synthesized sample powders was performed on a "DRON-SEIFERT-RM4" diffractometer ($\text{CuK}\alpha$ irradiation, graphite monochromator $d_{001} = 3.345 \text{ \AA}$, room temperature). The scanning range was $20^\circ - 55^\circ$ (2θ) with a step of 0.1° . The experimental diffraction data were processed using the PowderCell v.2.4 (Kraus and Nolze, 2000) and WINFIT 1.2.1 (Krumm, 1996) programs, which allowed a calculation of the quantitative phase composition, the lattice parameters, and the crystallite size (D_{XRD}). Data from the JCPDS-ICDD database (Powder Diffraction File, 2009) were used as reference. The composition of the $\text{Au}_x\text{Pd}_{1-x}$ alloys was determined using the experimentally measured dependence between lattice parameters of face-centered cubic cell (fcc, space group Fm-3m) in gold-palladium solid solutions and the atomic fraction of constituent elements (Shubin et al., 2012).

Transmission electron microscopy (TEM) study was performed using a JEM-2010 (lattice plane resolution 0.14 nm at accelerating voltage of 200 kV) equipped with an energy-dispersive X-ray (EDX) spectrometer EDAX [Si(Li) detector with 130 eV energy resolution]. The samples for the TEM study were prepared on perforated carbon film mounted on a copper grid.

Fourier transform infrared spectroscopy (FTIR) analysis of the catalyst samples was performed using Shimadzu IRAffinity spectrometer using KBr as a diluent.

X-ray photoelectron spectroscopic (XPS) analysis was performed using an ES-300 (KRATOS Analytical) photoelectron spectrometer. MgK α ($h\nu = 1253.6$ eV) X-ray source was applied for spectra registration. The spectrometer calibration was performed using bulk gold (Au4f $_{7/2}$) and copper (Cu2p $_{3/2}$) photoelectron lines with binding energy (BE) values of 84.0 and 932.7 eV, respectively. The position of the Si2p line for oxidized silicon with BE = 103.3 eV was used as reference for spectra calibration. Due to the overlapping of Au4d- and Pd3d- spectral regions (Smolentseva et al., 2011), the subtraction of Au4d line from Au/PSi sample was applied for all bimetallic catalysts to analyze palladium surface species precisely. The chemical composition of the surface was quantitatively determined from integral peak areas using standard atomic sensitivity factors (ASFs) (Wagner et al., 2013). Processing of the obtained data and spectral analyses were performed using homemade XPS-Calc program, which has been tested on a number of systems (Svintsitskiy et al., 2013). The curve fitting procedure was performed using an approximation based on a combination of the Gaussian and Lorentzian functions with the subtraction of a Shirley-type background. Before the curve fitting, all spectra were smoothed using a Fourier filter. No considerable difference between the smoothed and experimental curves was observed (standard deviation <1%).

RESULTS

Catalysts Characterization

Table 1 shows actual metal loading, specific surface area and pore volume of the prepared samples. The metal loading was close to the calculated value for all the samples studied. S_{BET} changed from 154 m 2 g $^{-1}$ for the pure PSi to 104 m 2 g $^{-1}$ for the PdAu $_2$ /PSi, respectively. V_p decreased synchronously with S_{BET} from 0.25 cm 3 g $^{-1}$ for the pure PSi to 0.17 cm 3 g $^{-1}$ for the PdAu $_2$ /PSi.

PSi contains surface H-terminal atoms, which can act as an internal surface reducing agent facilitating metal reduction. The presence of such H-terminal atoms in fresh (as received samples stored on air) non-oxidized PSi support and catalyst samples was monitored by FTIR. **Figure 2** shows IR-spectra of the PSi support before catalyst preparation and of Pd/PSi, Au/PSi, Pd-Au/PSi, and PdAu $_2$ /PSi catalysts. The PSi spectrum contains the

stretching modes of Si-H $_x$ bonds (2,082, 2,107, and 2,132 cm $^{-1}$ for $x = 1, 2,$ and $3,$ respectively) (Ogata et al., 2000; Polisski et al., 2010). The IR-spectra of the catalysts do not show stretching modes of Si-H $_x$ bonds, indicating that all H-terminal atoms were spent during catalysts preparation.

Figure 3 shows XRD patterns of the catalysts studied and of the PSi support. The silicon phase ($2\Theta = 47.30^\circ$) was identified for all the samples. For the Pd/PSi and the Au/PSi catalysts, metallic Pd ($2\Theta = 40.15^\circ$ and 46.70°) with the crystallite size (D_{XRD}) of 12 nm and Au ($2\Theta = 38.32^\circ$ and 44.62°) with the crystallite size of 5 nm, respectively, were identified, see also **Table 2**. The XRD pattern of Pd-Au/PSi contains not fully resolved peaks at $2\Theta = 40.08^\circ$ and 39.02° , which could be assigned to metallic Pd ($D_{\text{XRD}} = 6.3$ nm) and solid solution Pd $_{0.35}$ Au $_{0.65}$ ($D_{\text{XRD}} = 5.5$ nm). Bimetallic nanoparticles are gold-enriched compared to the data on elemental composition, **Table 1**, due to the presence of significant amount of monometallic Pd nanoparticles. The XRD pattern of PdAu $_2$ /PSi catalyst contains broad peaks at $2\Theta = 38.79^\circ$ and 45.01° , which could be assigned to the solid solution Pd $_{0.25}$ Au $_{0.75}$ nanoparticles with the crystallite size of 4 nm. The composition of Pd $_{0.25}$ Au $_{0.75}$ solid solution is relatively close to the stoichiometry of DCS and data on elemental composition, **Table 1**. Most likely, small enrichment by gold is caused by the presence of pure Pd particles, which is confirmed by the presence of a shoulder at the position of metallic Pd, **Figure 3**. The obtained data allows us to estimate that ca. 2/3 $^{\text{s}}$ of Pd in the PdAu $_2$ /PSi catalyst is present in the form of bimetallic particles, while 1/3 $^{\text{rd}}$ is present in the form of pure Pd. Assuming the similar particle size and taking into account the significant dilution by gold in the bimetallic particles the quantitative ratio of bimetallic to pure Pd particles in the catalyst could be estimated to be not < 8, thus indicating that the majority of particles are bimetallic.

PdAu $_2$ /PSi and Pd-Au/PSi catalysts were studied by TEM and EDX. PdAu $_2$ /PSi contains agglomerates of bimetallic nanoparticles with the sizes in the range of 5–10 nm, see **Figures 4a,b**. According to the EDX data, composition of the nanoparticles is non-uniform: some particles are enriched by Pd. However, the average composition of agglomerates is close to Pd $_{0.25}$ Au $_{0.75}$, that was also identified by the XRD. **Figures 4c,d** show that Pd-Au/PSi also contains the agglomerates of bimetallic nanoparticles with the sizes in the range of 3–20 nm. The composition of nanoparticles is non-uniform and varies from pure Pd to Au-enriched alloys. The peaks of Pd-Au alloys at XRD patterns of PdAu $_2$ /PSi and Pd-Au/PSi catalysts have a certain

TABLE 1 | Catalyst's metal loading, specific BET surface area and pore volume.

Catalyst	Precursor	S_{BET} , m 2 /g	V_p , cm 3 /g	Pd, wt. %	Au, wt. %	Pd/(Pd+Au) atomic ratio
PSi	–	154	0.25	0	0	–
Au/PSi	H[AuCl $_4$]	133	0.20	0	5	1
Pd/PSi	[Pd(NH $_3$) $_4$](NO $_3$) $_2$	141	0.20	2.1	0	0
Pd-Au/PSi	H $_2$ [PdCl $_4$]+H[AuCl $_4$]	127	0.19	2.1	2	0.66
PdAu $_2$ /PSi	[Pd(NH $_3$) $_4$][AuCl $_4$] $_2$	104	0.17	1.9	7.3	0.33

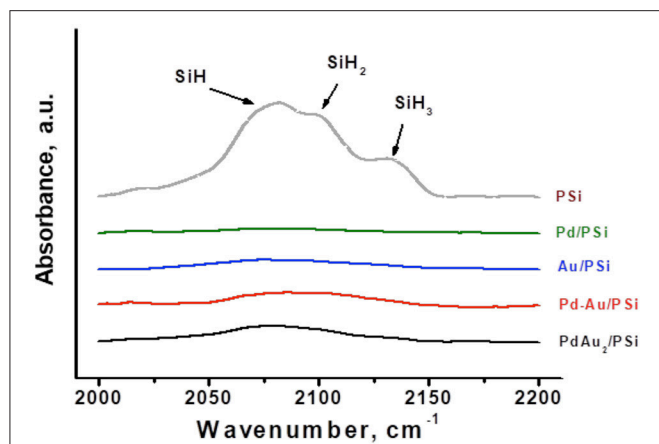


FIGURE 2 | The IR-spectra of PSi support and Pd/PSi, Au/PSi, Pd-Au/PSi, and PdAu₂/PSi catalysts.

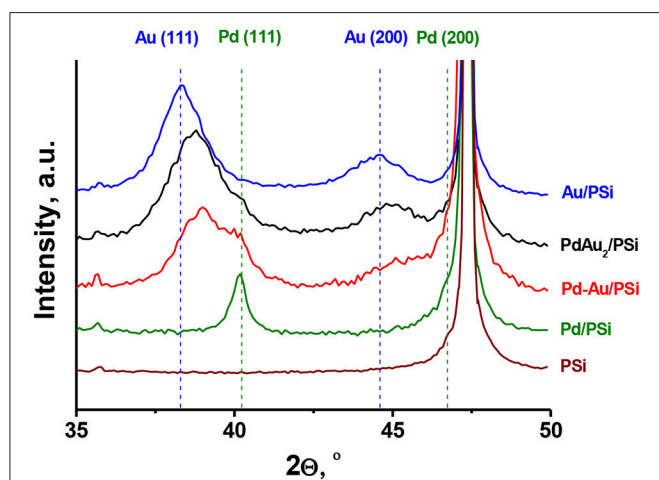


FIGURE 3 | XRD patterns of PSi support and Pd/PSi, Au/PSi, Pd-Au/PSi, and PdAu₂/PSi catalysts.

TABLE 2 | Catalysts phase composition, relating to **Figure 3**.

Catalyst	Phase composition	Crystallite size (D_{XRD}), nm
Au/PSi	Au	5
Pd/PSi	Pd	12
Pd-Au/PSi	Pd _{0.35} Au _{0.65}	5.5
	Pd	6.3
PdAu ₂ /PSi	Pd _{0.25} Au _{0.75}	4

degree of asymmetry, indicating the non-uniformity of alloy nanoparticles composition, in a good agreement with EDX data. The analysis of distribution of particles composition and complex XRD fitting requires much wider array of TEM and EDX data and is out of the scope of this work. However, the majority of metallic particles in Pd-Au/PSi and practically all in PdAu₂/PSi catalysts are bimetallic.

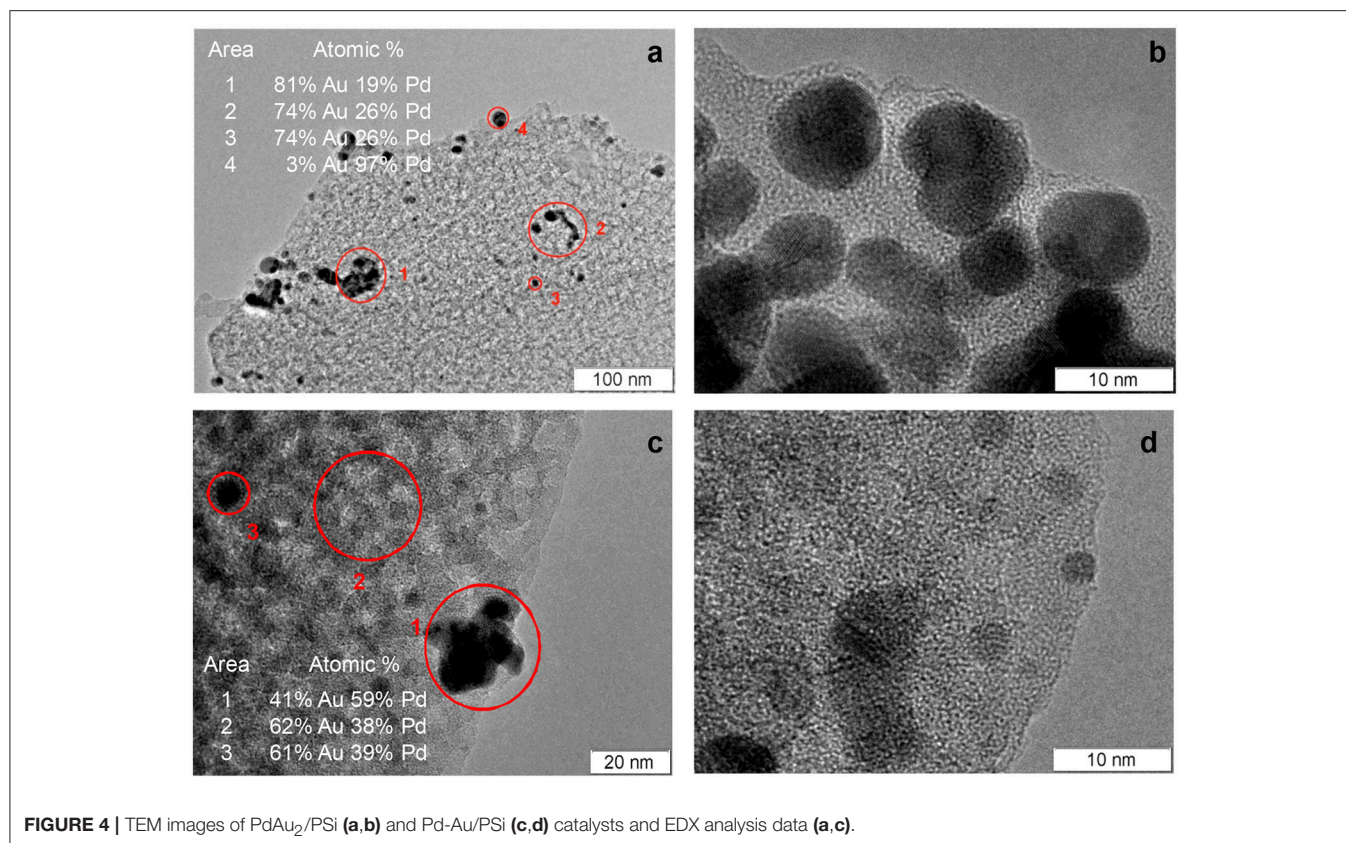
Figure 5 shows the X-ray photoelectron spectra of the bimetallic Pd-Au catalysts in comparison with the monometallic Pd/PSi and Au/PSi samples. Spectral Si2p-regions were the same for all studied samples and consisted of three components with BE(Si2p) of ~99, 101 and 103.3 eV. According to the literature data, Si2p peaks with BE ~99 and 103.3 eV can be attributed to Si⁰ and oxidized Si⁴⁺ (SiO₂-type) species, respectively (Wagner et al., 2013). The position of oxidized Si⁴⁺ peak was found to be stable during spectra registration and was chosen as a reference for spectra calibration. The Si2p peak with BE ~101 eV was characterized by the lowest intensity and could be interpreted as an interface SiO_x between silicon and surface oxidized SiO₂-type layer. The quantitative ratio between different silicon states is given in **Table 3**. Therefore, surface of porous silicon used as a support material was found to be partially oxidized, which is expected for PSi materials not stored in an oxygen-free environment.

Quantitative XPS analysis has also shown that surface Pd amount was similar for bimetallic and monometallic samples (Pd/Si~0.013), while gold amount was found to be lower for bimetallic catalyst (Au/Si~0.006 and 0.0025) than for Au/PSi (Au/Si~0.031). This indicates enrichment of the surface of the bimetallic samples by palladium. Surface palladium enrichment can be caused by interaction with oxygen followed by formation of the oxidized palladium species (Hilaire et al., 1981). As seen from **Figure 5**, two doublet components with BE ~335.2 and 336.6 eV identified as Pd3d_{5/2} were observed in Pd3d spectra for all studied samples. The doublet with BE ~335.2 eV can be attributed to metallic palladium, while the second Pd3d component is caused by the presence of oxidized Pd²⁺ state, probably, in PdO form (Smolentseva et al., 2011). Hence, the observed segregation of palladium can be related to the process of surface oxidation. The amount of Pd²⁺ was similar for all the studied catalysts and equal to ca. 30%, see **Table 3**.

Detailed XPS analysis of the Au-containing samples showed presence of two Au4f doublet components with BE ~83.7 and 85.1 eV (Au4f_{7/2}). These were attributed to metallic Au⁰ and weakly oxidized Au^{δ+} species, respectively (Ballester et al., 2015).

Results of the analysis of the catalysts' surface composition reveal that the surface of the bimetallic Pd-Au nanoparticles is enriched by Pd atoms present in Pd⁰ and Pd²⁺ states. It should be noted that according to literature (Ouyang et al., 2015) the presence of both, Pd⁰ and PdO, forms on the catalysts surface is required for the catalysts to be active in direct synthesis of H₂O₂.

One can conclude that the Pd-Au/PSi catalyst prepared by the conventional H₂[PdCl₄] and H[AuCl₄] precursors contains monometallic Pd and a wide range of different Pd-Au solid solution nanoparticles over the oxidized PSi surface, whereas the PdAu₂/PSi catalyst prepared by [Pd(NH₃)₄][AuCl₄]₂ DCS single-source precursor reduction predominantly contains bimetallic Pd-Au solid solution nanoparticles with the composition close to Pd_{0.25}Au_{0.75}. For both catalysts surface of bimetallic nanoparticles is Pd-enriched and contains palladium in Pd⁰ and Pd²⁺ states.



H₂O₂ Direct Synthesis

The PSi supported catalysts were tested in H₂O₂ direct synthesis at T = −10°C and P = 1 bar in a batch reactor with bubbling H₂-O₂ gas mixture and 0.03 M H₂SO₄ methanol solution as a reaction media. Methanol could be suggested as one of the best solvents for this reaction due to high H₂ and O₂ solubilities, inability to form dangerous organic peroxides and the fact that it is a favorable solvent for many oxidation reactions involving H₂O₂ (Melada et al., 2006), such as propylene epoxidation process (Biasi et al., 2013).

After each catalytic test the catalyst powder was filtered and the residual reaction media was tested in the reaction conditions for 1 h in order to check metal leaching from the catalysts. None of the filtrates showed any activity in H₂O₂ synthesis or decomposition, indicating that PSi-supported metallic nanoparticles were stable under the reaction conditions tested, or leached metals were inactive in any relevant catalytic reactions. Filtered catalyst powders were recycled to the 2nd 3 h long catalytic run and properties of all catalysts were fully reproduced with respect to amount of catalyst recycled.

Figure 6 shows the time course of H₂O₂ concentration (Figure 6A), H₂ conversion (Figure 6B) and selectivity (Figure 6C) for the direct H₂O₂ synthesis over Pd/PSi, Au/PSi, Pd-Au/PSi, and PdAu₂/PSi catalysts. It is seen that the Au/PSi catalyst was inactive in the direct H₂O₂ synthesis as well as in complete H₂ oxidation: H₂ conversion was < 4%. The Pd-containing catalysts were active in the direct H₂O₂

synthesis. For all the Pd-based catalysts H₂O₂ concentration grows nearly linearly with time, H₂ conversion is constant, while selectivity slowly decreases. The H₂O₂ concentration of ca. 6 mM was reached over Pd/PSi after 5 h on stream at X_{H₂} of 10% and S_{H₂O₂} decrease from 25 to 20%. The Pd-Au/PSi catalyst was more active: [H₂O₂] of ca. 9 mM was reached after 5 h on stream at X_{H₂} of 15% and S_{H₂O₂} decrease from 25 to 20%. The Pd/PSi and Pd-Au/PSi catalysts exhibited similar selectivity vs. time dependencies. This could be associated with the presence of monometallic Pd nanoparticles in both catalysts. Higher activity of Pd-Au/PSi could be associated with higher metal dispersion.

The PdAu₂/PSi catalyst exhibited the best performance in the direct H₂O₂ synthesis. H₂O₂ concentration of ca. 23 mM was reached after 5 h on stream at X_{H₂} of 23% and S_{H₂O₂} decreases from ca. 50 to ca. 45%. High activity of PdAu₂/PSi in H₂ oxidation could be associated with high metal dispersion (4 nm for PdAu₂/PSi vs. 5–6 nm for Pd-Au/PSi vs. 12 nm for Pd/PSi), while high selectivity toward H₂O₂ synthesis could be associated with the major part of Pd in the catalyst being in the form of bimetallic Pd-Au nanoparticles, since monometallic Pd nanoparticles are known to be active in the undesirable H₂O₂ hydrogenation reaction. The obtained data on H₂O₂ direct synthesis shows that bimetallic PSi-supported catalysts are more active and selective (in the case of PdAu₂/PSi), compared with the monometallic Pd/PSi, which is not surprising (Edwards et al., 2015; Li and Yoshizawa, 2015).

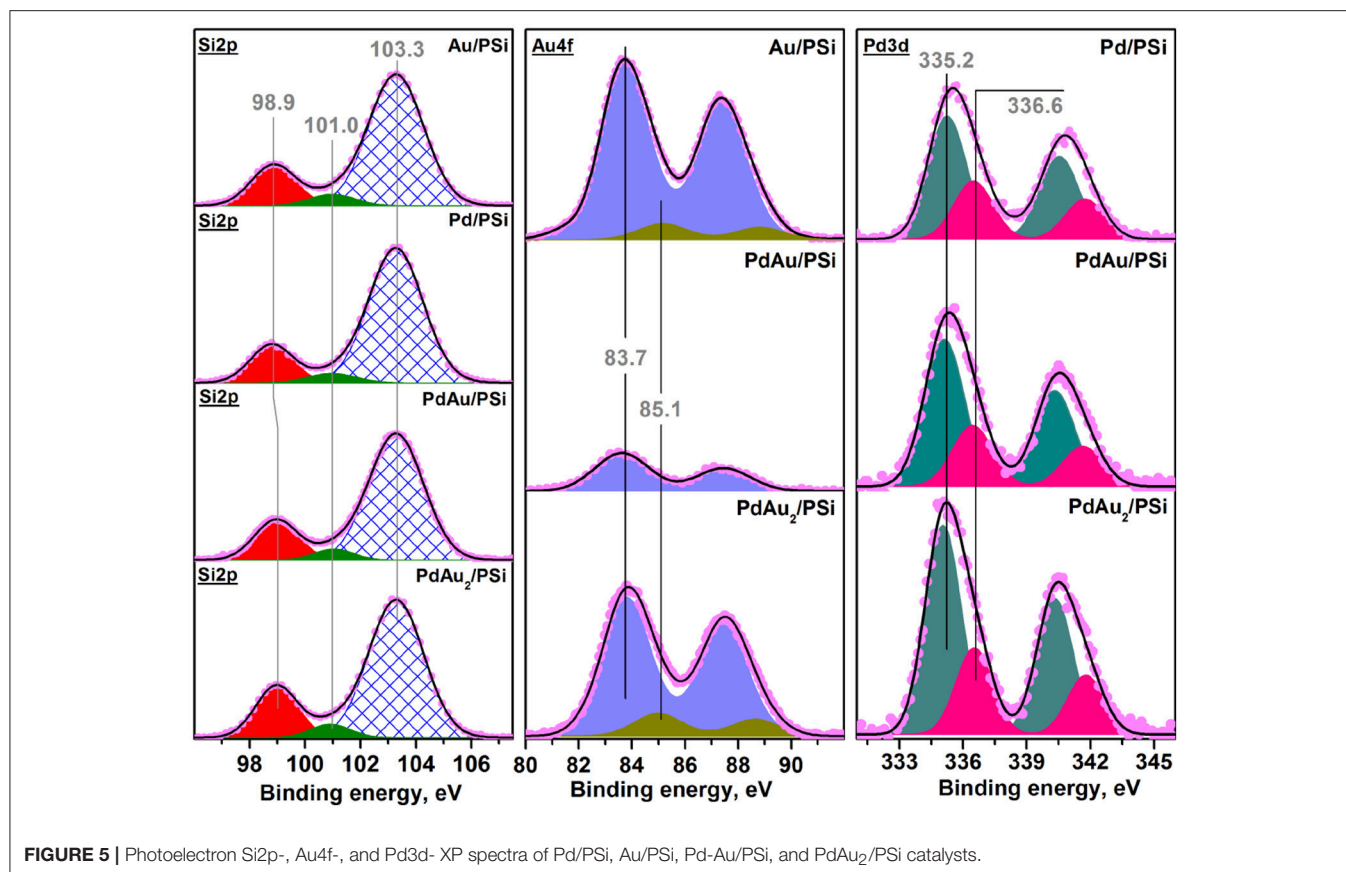


TABLE 3 | XPS data on the surface composition of the catalysts.

Catalyst	Pd/PSi	Au/PSi	Pd-Au/PSi	PdAu ₂ /PSi
(Pd/Si)·10 ²	1.3	–	1.1	1.4
(Au/Si)·10 ²	–	3.1	0.6	2.5
Pd/Au	–	–	1.8	0.6
Pd ²⁺ , %	31	–	27	29
Au ³⁺ , %	–	8	–	13
Si ⁰ , %	18	20	19	22
SiO _x , %	5	6	6	5
Si ⁴⁺ , %	77	75	75	73

It was shown, that for Pd/PSi, Pd-Au/PSi, and PdAu₂/PSi catalysts selectivity of H₂O₂ synthesis slowly decreased with time, while H₂ conversion remained constant (Figures 6B,C). It could be caused by the occurrence of the undesirable H₂O₂ decomposition and hydrogenation reactions. In order to elucidate the influence of these reactions the H₂O₂ decomposition and hydrogenation reactions were studied over PSi-supported catalysts.

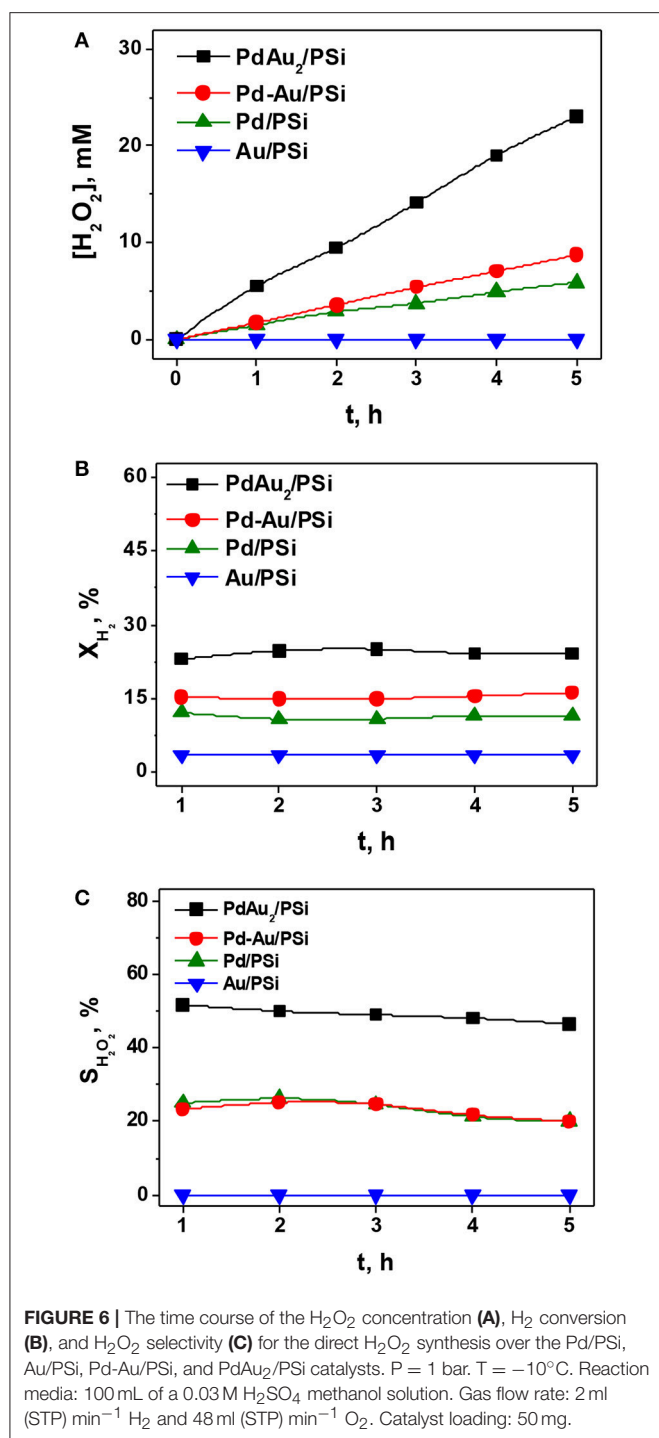
H₂O₂ Decomposition and Hydrogenation

In order to study stability of the synthesized H₂O₂ at the reaction conditions a number of experiments on H₂O₂ decomposition and hydrogenation were carried out. Experimental conditions

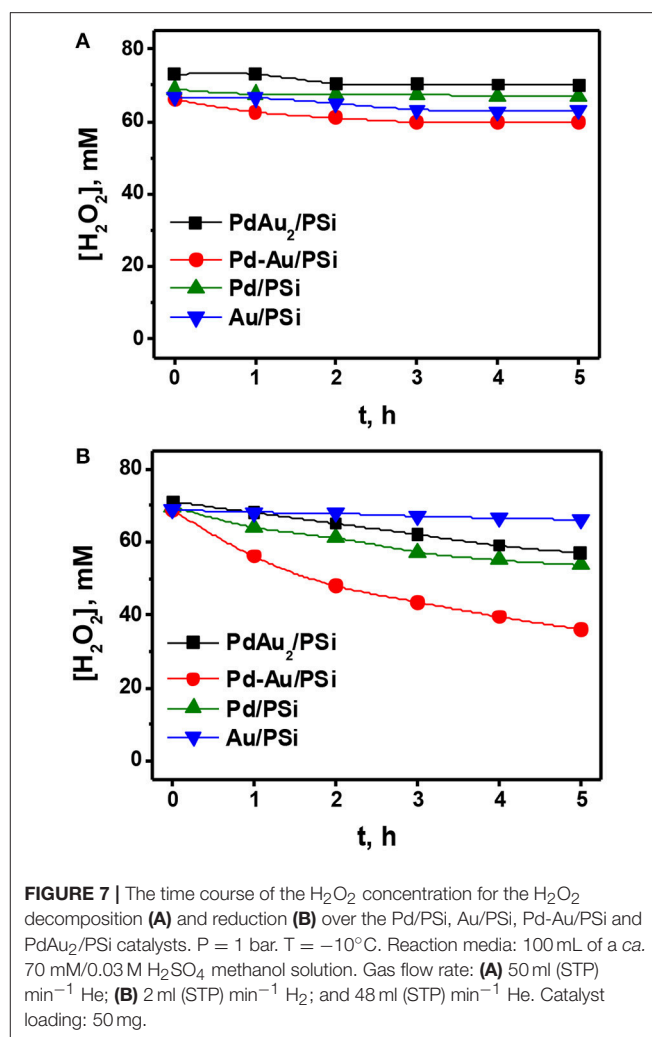
were close to that for H₂O₂ synthesis in this work. As initial reaction media 0.07 M H₂O₂/0.03 M H₂SO₄ methanol solution was chosen. The reactions were carried out at –10°C.

At first, the reaction of H₂O₂ decomposition was studied. Figure 7A shows the time course of H₂O₂ concentration for H₂O₂ decomposition over Pd/PSi, Au/PSi, Pd-Au/PSi, and PdAu₂/PSi catalysts. It is seen, that H₂O₂ concentration was constant for the Pd/PSi, Au/PSi, and PdAu₂/PSi catalysts and negligibly decreased in the case of Pd-Au/PSi. This indicates that all studied catalysts were generally inactive in H₂O₂ decomposition.

Figure 7B shows the results on H₂O₂ hydrogenation over the Pd/PSi, Au/PSi, Pd-Au/PSi, and PdAu₂/PSi catalysts. It is seen, that H₂O₂ concentration was practically constant during 5 h over Au/PSi, indicating that Au/PSi was practically inactive in H₂O₂ hydrogenation. Over Pd/PSi and PdAu₂/PSi catalysts H₂O₂ concentration slowly decreased from 70 mM to ca. 55 mM after 5 h on stream. Pd-Au/PSi was the most active one in H₂O₂ hydrogenation: H₂O₂ concentration decreased from 70 to 36 mM after 5 h on stream. The differences in behavior of the Pd-based catalysts are caused by the different phase compositions and dispersions of the active component. The PdAu₂/PSi catalyst was less active in H₂O₂ hydrogenation than Pd-Au/PSi and Pd/PSi despite the higher metal dispersion due to the presence of the major part of Pd in the catalyst in the form of bimetallic Pd-Au nanoparticles.



Thus, one can conclude that, unlike H₂O₂ decomposition, H₂O₂ hydrogenation significantly influences direct H₂O₂ synthesis over the Pd/PSi, Pd-Au/PSi and PdAu₂/PSi catalysts, decreasing reaction selectivity and limiting the maximum reachable H₂O₂ concentration. Among the catalysts studied the PdAu₂/PSi is the least active in H₂O₂ hydrogenation.



DISCUSSION

Among the catalysts studied in the present work the PdAu₂/PSi one showed the highest activity and selectivity in the direct synthesis of H₂O₂. This is due to its high activity in H₂O₂ synthesis reaction as well as low activity in the undesirable H₂O₂ decomposition and hydrogenation side reactions. We assign excellent performance of the PdAu₂/PSi catalyst to the fact that most of Pd in the catalyst is in the form of bimetallic Pd-Au nanoparticles. The preferred method of synthesis of supported bimetallic Pd-Au nanoparticles was found to be based on DCS [Pd(NH₃)₄][AuCl₄]₂ reduction inside the PSi's pore space by the surface H-terminal atoms. The alloy nanoparticles are the primary product of DCS reduction. Prevention of intermediate formation of monometallic Pd and Au grains allows one to obtain bimetallic nanoparticles under very mild conditions. The composition of the formed Au_{0.75}Pd_{0.25} nanoparticles is relatively close to the DCS stoichiometry. Thus, it could be concluded, that the presence of specific chemical interaction between the Pd and Au precursors

promotes formation of supported bimetallic nanoparticles and, therefore, active and selective catalyst, while the application of conventionally used joint water solutions of Pd and Au chlorides leads to the formation of a wide range of different Pd-Au bimetallic nanoparticles as well as pure Pd and Au ones (e.g., the case of Pd-Au/PSi) (Edwards et al., 2009).

Despite the fact that surface of as received PSi was H-terminated, the surface of as-prepared catalysts was mostly covered by a SiO₂ layer. From one side it presents the possibility for strong metal-support interaction (SMSI) in the Pd_xAu_{1-x}-PSi system, which is generally favorable for H₂O₂ direct synthesis catalysts due to electron transfer from Pd (Yi et al., 2016). However, the SMSI effect in the Si-based systems is typically observed after high temperature reduction and is associated with silicide phases or layers formation (Ueckert et al., 1997). This is not the case here. From the other side SiO₂ is an acidic support with low value of surface isoelectric point of about 2, which is desirable for stabilization of the formed H₂O₂. Also, the SiO₂ layer encapsulates the possible undesirable contaminations and provides the material inertness with respect to H₂O₂ decomposition and hydrogenation reactions.

Gemo et al. (2015) and Ouyang et al. (2015) highlighted the key role of Pd²⁺/Pd⁰ surface ratio on the Pd catalysts performance in the direct synthesis of H₂O₂. Simultaneous presence of Pd⁰ and Pd²⁺ sites at the surface is required to provide dissociative H₂ adsorption and non-dissociative O₂ adsorption. The single-metal Pd catalysts tend to oxidation under reaction conditions that is undesirable (Gemo et al., 2015). High values of H₂⁺/Pd ratio (H₂⁺—the concentration of hydrogen dissolved in liquid media) and Pd particle size increase lead to the stabilization of Pd⁰ surface sites. We believe that Au addition to Pd together with selective formation of Pd-Au bimetallic particles increases its resistance toward oxidation as Au is a “very noble” metal. The Pd-Au particle size in the PdAu₂/PSi catalyst is not very small. All these factors protect Pd surface from deep oxidation under reaction conditions and help to provide the acceptable Pd²⁺/Pd⁰ surface ratio and reach higher H₂O₂ selectivity.

The properties of PdAu₂/PSi in direct H₂O₂ synthesis were compared with other Pd-based catalytic systems. **Table 4** summarizes the literature data on catalytic performance and reaction conditions. PdAu₂/PSi catalyst studied in the present work showed the H₂O₂ productivity of 0.5 mol g_{Pd}⁻¹ h⁻¹ or 12.3 mol kg_{cat}⁻¹ h⁻¹ at selectivity of 50%, that is lower than the productivity of the best-known catalysts. The lower H₂O₂ production rate could be associated with low reaction temperature of -10°C. The highest values of productivity were obtained for Pd_{0.1}Au_{0.0333}Cs_{2.5}H_{0.2}PW₁₂O₄₀ (29.4 mol g_{Pd}⁻¹ h⁻¹) (Ntainjua et al., 2012) and Pd-Au/C (6.4 mol g_{Pd}⁻¹ h⁻¹) (Edwards et al., 2009) catalysts. However, these studies utilized elevated pressures of 40 and 37 atm, respectively. In the works Bernardotto et al. (2009) and Ouyang et al. (2015), the experiments were carried at atmospheric pressure and the productivity values of 3.0 mol g_{Pd}⁻¹ h⁻¹ for Pd/TiO₂

TABLE 4 | The comparison of catalyst performance and reaction conditions for direct H₂O₂ synthesis over different Pd-based systems.

Catalyst	T, °C	P, bar	Gas composition	Solvent	S _{H₂O₂} , %	Productivity, mol _{H₂O₂} /kg _{cat} ·h	Productivity, mol _{H₂O₂} /g _{Pd} ·h	Maximum reached [H ₂ O ₂], wt. %	References.
PdAu ₂ /PSi	-10	1	96 O ₂ , 4 H ₂	H ₂ SO ₄ , CH ₃ OH	50	12.3	0.5	0.1 ^a	This work
Pd/TiO ₂	10	1	60 O ₂ , 15H ₂ , 25 N ₂	H ₂ SO ₄ , C ₂ H ₅ OH	60	29.9	3.0	-	Ouyang et al., 2015
PdAu ₂ /ZrO ₂	25	1	96 O ₂ , 4 H ₂	H ₂ SO ₄ , CH ₃ OH	60	13.7	1	0.4 ^a	Bernardotto et al., 2009
Pd-Au/TiO ₂	2	37	7 O ₂ , 3.5 H ₂ , 89.5CO ₂	H ₂ O, CH ₃ OH	60	64	2.9	0.6 ^b	Edwards et al., 2005
Pd _{0.1} Au _{0.0333} Cs _{2.5} H _{0.2} PW ₁₂ O ₄₀	2	40	7 O ₂ , 3.5 H ₂ , 89.5 CO ₂	H ₂ O, CH ₃ OH	-	97	29.4	0.3	Ntainjua et al., 2012
Pd-Au/C	2	37	7 O ₂ , 3.5 H ₂ , 89.5 CO ₂	H ₂ O, CH ₃ OH	98	160	6.4	1.0	Edwards et al., 2009

^aAfter 5 h on stream.

^bAfter 12 h on stream.

(Svintsitskiy et al., 2013) and $1.0 \text{ mol g}_{\text{Pd}}^{-1} \text{ h}^{-1}$ for PdAu₂/ZrO₂ (Bernardotto et al., 2009) were obtained. These are closer to the results obtained for the PdAu₂/PSi catalyst, taking into account the higher reaction temperatures: 10°C for Pd/TiO₂ and 25°C for PdAu₂/ZrO₂. Also, similar selectivities were obtained: 60% for Pd/TiO₂ and PdAu₂/ZrO₂ vs. 50% for PdAu₂/PSi.

As indicated above, the minimal required H₂O₂ concentration produced by direct synthesis for practical applications is estimated to be 1 wt.% or 0.23 M in a methanol solution (Garcia-Serna et al., 2014). In Edwards et al. (2005) and Ntainjua et al. (2012) the maximum reached H₂O₂ concentration was ca. 0.3 wt.% and was limited by the reaction of H₂O₂ hydrogenation. The perfectly selective Pd-Au/C catalyst allowed to reach H₂O₂ concentration of more than 1.0 wt.% by several gas top-ups in a closed batch system at 37 bar pressure and 2°C (Edwards et al., 2009). The closer conditions of atmospheric pressure and flowing gas feed were utilized in Bernardotto et al. (2009) and H₂O₂ concentrations of 0.4 and 0.6 wt.% were reached after 5 and 12 h on stream, respectively. Thus, the target of 1.0 wt.% was likely achievable. In the present work the maximum H₂O₂ concentration reached is 0.1 wt.% after 5 h on stream, which is less than that of the best catalysts. The estimation of H₂O₂ synthesis and hydrogenation rates for PdAu₂/PSi catalyst gives the maximum achievable H₂O₂ concentration at the level of ca. 0.8 wt.%, which could be reached by increasing reaction time and/or catalyst loading.

Thus, it is clear, that further catalyst improvement is required. However, even at this point of development it is clear, that PSi supported bimetallic Pd-Au system is a promising system to be used in the continuous flow systems for direct H₂O₂ synthesis. Applying the electrochemical etching technique, a layer of porous silicon could be fabricated directly on the silicon microchannel's surface and used as a support (Drott et al., 1997) for Pd-Au catalyst, avoiding the need of laborious catalyst deposition procedure. If so, silicon microreactors with a porous silicon layer onto the channel walls with deposited Pd-Au nanoparticles is a very intriguing option for performing H₂O₂ direct synthesis due to enhanced control abilities (Srinivas et al., 2004; Huang et al., 2014), possibility of safe operation at high temperatures and pressures (Divins et al., 2011) and wide range of reactor geometries available.

CONCLUSIONS

In conclusion, we would like to point out key features of DCS application as a precursor and porous silicon as a support for direct H₂O₂ synthesis catalysts:

REFERENCES

Ballesterio, D., Juan, R., Ibarra, A., Gómez-Giménez, C., Ruiz, C., Rubio, B., et al. (2015). Effect of thermal treatments on the morphology, chemical state and lattice structure of gold nanoparticles deposited onto carbon structured monoliths. *Colloids Surf. A* 468, 140–150. doi: 10.1016/j.colsurfa.2014.12.017

- The DCS [Pd(NH₃)₄][AuCl₄]₂ reduction inside the pore space of the support promotes the selective formation of Pd-Au alloy nanoparticles under very mild conditions.
- The composition of formed supported bimetallic Pd-Au nanoparticles is close to the stoichiometry of DCS.
- The Pd-Au catalysts prepared by DCS [Pd(NH₃)₄][AuCl₄]₂ reduction is active in direct H₂O₂ synthesis.
- PSi is porous material that could effectively enhance dispersion of supported metal nanoparticles.
- PSi with partially oxidized surface is an inert material with respect to undesirable H₂O₂ decomposition and hydrogenation reactions and thus could be used as a catalysts support for direct H₂O₂ synthesis reaction.
- The surface of PSi-supported catalysts is coated by Si⁰ and SiO₂ sites and thus PSi could be easily wetted by different solvents, such as water, methanol, ethanol, and others.
- PSi supported Pd-Au catalysts are quite active and selective in direct H₂O₂ synthesis.
- PSi's surface H-terminal atoms could effectively reduce different Pd and Au precursors with the formation of bimetallic Pd-Au alloy nanoparticles. Thus bimetallic Pd-Au nanoparticles could be easily deposited onto already established PSi layer.
- PSi is a promising support for direct hydrogen peroxide synthesis from engineering point of view due to its high thermal stability and conductivity, possibility of safe operation at high temperatures and pressures, and well-established silicon processing techniques, providing the possibility to design reactors of complex internal geometry with surface porous silicon layers.

AUTHOR CONTRIBUTIONS

DP: catalytic experiments, overall results analysis; DM: catalytic experiments; KL: FTIR experiments; PS: catalyst preparation, BET analysis; YS: XRD analysis; PP: precursors preparation, ICP AES analysis; DS: XPS analysis; VS: results analysis; AL: concept of PSi-supported catalysts, supervision of catalyst testing, and manuscript preparation and editing.

ACKNOWLEDGMENTS

The authors are grateful to Dr. V. I. Zaikowskii for assistance in HRTEM analysis. The work was supported by RFBR Grant 16-33-60106_mol_a_dk. This research was, in part, supported by the National Research Foundation, Prime Minister's Office, Singapore, under its CREATE program. We gratefully acknowledge inspiration to work with porous silicon from our former colleague, late Professor DK.

Bavykin, D. V., Lapkin, A. A., Plucinski, P. K., Friedrich, J. M., and Walsh, F. C. (2005). TiO₂ nanotube supported ruthenium (III) hydrated oxide: a highly active catalyst for selective oxidation of alcohols with oxygen. *J. Catal.* 235, 10–17. doi: 10.1016/j.jcat.2005.07.012

Bernardotto, G., Menegazzo, F., Pinna, F., Signoretto, M., Cruciani, G., and Strukul, G. (2009). New Pd–Pt and Pd–Au catalysts for an efficient synthesis

- of H₂O₂ from H₂ and O₂ under very mild conditions. *Appl. Catal. A* 358, 129–135. doi: 10.1016/j.apcata.2009.02.010
- Biasi, P., Garcia-Serna, J., Bittante, A., and Salmi, T. (2013). Direct synthesis of hydrogen peroxide in water in a continuous trickle bed reactor optimized to maximize productivity. *Green Chem.* 15, 2502–2513. doi: 10.1039/c3gc40811f
- Bulushev, D. A., Beloshapkin, S., Plyusnin, P. E., Shubin, Y. V., Bukhtiyarov, V. I., Korenev, S. V., et al. (2013). Vapour phase formic acid decomposition over PdAu/γ-Al₂O₃ catalysts: effect of composition of metallic particles. *J. Catal.* 299, 171–180. doi: 10.1016/j.jcat.2012.12.009
- Climent, M. J., Corma, A., Iborra, S., and Sabater, M. J. (2014). Heterogeneous catalysis for tandem reactions *ACS Catal.* 4, 870–891. doi: 10.1021/cs401052k
- Coulthard, I., and Sham, T. K. (1998). Novel preparation of noble metal nanostructures utilising porous silicon. *Solid State Commun.* 105, 751–754. doi: 10.1016/S0038-1098(97)10229-0
- Coulthard, I., de Jiang, T., Lorimer, J. W., Sham, T. K., and Feng, X. H. (1993). Reductive deposition of Pd on porous silicon from aqueous solutions of PdCl₂: an X-ray absorption fine structure study. *Langmuir* 9, 3441–3445. doi: 10.1021/la00036a018
- Coulthard, I., Sammynaiken, R., Naftel, S. J., Zhang, P., and Sham, T. K. (2000). Porous silicon: a template for the preparation of nanophase metals and bimetallic aggregates. *Phys. Stat. Sol. A* 182, 157–162. doi: 10.1002/1521-396X(200011)182:1<157::AID-PSSA157>3.0.CO;2-O
- Dasog, M., Kraus, S., Sinelnikov, R., Veinot, G. C., and Rieger, B. (2017). CO₂ to methanol conversion using hydride terminated porous silicon nanoparticles. *Chem. Commun.* 53, 3114–3117. doi: 10.1039/C7CC00125H
- Dhakshinamoorthy, A., Opanasenko, M., Cejka, J., and Garcia, H. (2013). Metal organic frameworks as heterogeneous catalysts for the production of fine chemicals. *Catal. Sci. Technol.* 3, 2509–2540. doi: 10.1039/c3cy00350g
- Dittmeyer, R., Grunwaldt, J. D., and Pashkova, A. (2015). A review of catalyst performance and novel reaction engineering concepts in direct synthesis of hydrogen peroxide. *Catal. Today* 248, 149–159. doi: 10.1016/j.cattod.2014.03.055
- Divins, N. J., López, E., Roig, M., Trifonov, T., Rodríguez, A., de Rivera, F. G., et al. (2011). A million-channel CO-PrOx microreactor on a fingertip for fuel cell application. *Chem. Eng. J.* 167, 597–602. doi: 10.1016/j.cej.2010.07.072
- Drott, J., Lindström, K., Rosengren, L., and Laurell, T. (1997). Porous silicon as the carrier matrix in microstructured enzyme reactors yielding high enzyme activities. *J. Micromech. Microeng.* 7, 14–23. doi: 10.1088/0960-1317/7/1/004
- Edwards, J. K., Freakley, S. J., Lewis, R. J., Pritchard, J. C., and Hutchings, G. J. (2015). Advances in the direct synthesis of hydrogen peroxide from hydrogen and oxygen. *Catal. Today* 248, 3–9. doi: 10.1016/j.cattod.2014.03.011
- Edwards, J. K., Pritchard, J., Piccinini, M., Shaw, G., He, Q., Carley, A. F., et al. (2012). The effect of heat treatment on the performance and structure of carbon-supported Au–Pd catalysts for the direct synthesis of hydrogen peroxide. *J. Catal.* 292, 227–238. doi: 10.1016/j.jcat.2012.05.018
- Edwards, J. K., Solsona, B. E., Landon, P., Carley, A. F., Herzing, A., Kiely, C. J., et al. (2005). Direct synthesis of hydrogen peroxide from H₂ and O₂ using TiO₂-supported Au–Pd catalysts. *J. Catal.* 236, 69–79. doi: 10.1016/j.jcat.2005.09.015
- Edwards, J. K., Solsona, B., Ntainjua, E., Carley, A. F., Herzing, A. A., Kiely, C. J., et al. (2009). Switching off hydrogen peroxide hydrogenation in the direct synthesis process. *Science* 323, 1037–1041. doi: 10.1126/science.1168980
- Ensafi, A. A., Jafari-Asl, M., Rezaei, B., Abarghoui, M. M., and Farrokhpour, H. (2015). Facile synthesis of Pt–Pd@Silicon nanostructure as an advanced electrocatalyst for direct methanol fuel cells. *J. Power Sources* 282, 452–461. doi: 10.1016/j.jpowsour.2015.02.065
- Fan, X., Zhang, G., and Zhang, F. (2015). Multiple roles of graphene in heterogeneous catalysis. *Chem. Soc. Rev.* 44, 3023–3035. doi: 10.1039/C5CS00094G
- Flytzani-Stephanopoulos, and Gates, B. C. (2012). Atomically dispersed supported metal catalysts. *Annu. Rev. Chem. Biomol. Eng.* 3, 545–574. doi: 10.1146/annurev-chembioeng-062011-080939
- Freakley, S. J., He, Q., Harrhy, J. H., Lu, L., Crole, D. A., Morgan, D. J., et al. (2016). Palladium-tin catalysts for the direct synthesis of H₂O₂ with high selectivity. *Science* 351, 965–968. doi: 10.1126/science.125705
- Freakley, S. J., Piccinini, M., Edwards, J. K., Ntainjua, E. N., Moulijn, J. A., and Hutchings, G. J. (2013). Effect of reaction conditions on the direct synthesis of hydrogen peroxide with a AuPd/TiO₂ catalyst in a flow reactor. *ACS Catal.* 3, 487–501. doi: 10.1021/cs400004y
- Garcia-Serna, J., Moreno, T., Biasi, P., Cocero, M. J., Mikkola, J.-P., and Salmi, T. O. (2014). Engineering in direct synthesis of hydrogen peroxide: targets, reactors and guidelines for operational conditions. *Green Chem.* 16, 2320–2343. doi: 10.1039/c3gc41600c
- Gemo, N., Sterchele, S., Biasi, P., Centomo, P., Canu, P., Zecca, M., et al. (2015). The influence of catalyst amount and Pd loading on the H₂O₂ synthesis from hydrogen and oxygen. *Catal. Sci. Technol.* 5, 3545–3555. doi: 10.1039/C5CY00493D
- Gu, J., Wang, S., He, Z., Han, Y., and Zhang, J. (2016). Direct synthesis of hydrogen peroxide from hydrogen and oxygen over activated-carbon-supported Pd-Ag alloy catalysts. *Catal. Sci. Technol.* 6, 809–817. doi: 10.1039/C5CY00813A
- Hilaire, L., Légaré, P., Holl, Y., and Maire, G. (1981). Interaction of oxygen and hydrogen with Pd-Au alloys: an AES and XPS study. *Surf. Sci.* 103, 125–140. doi: 10.1016/0039-6028(81)90103-5
- Huang, C. C., Huang, Y. J., Wang, H. S., Tseng, F. G., and Su, Y. C. (2014). A well-dispersed catalyst on porous silicon micro-reformer for enhancing adhesion in the catalyst-coating process. *Int. J. Hydrogen Ener.* 39, 7753–7764. doi: 10.1016/j.ijhydene.2014.03.029
- Hulkoti, N. I., and Taranath, T. C. (2014). Biosynthesis of nanoparticles using microbes — a review. *Colloids Surf. B Biointerfaces* 121, 474–483. doi: 10.1016/j.colsurfb.2014.05.027
- Julkapli, N. M., and Bagheri, S. (2015). Graphene supported heterogeneous catalysts: an overview. *Int. J. Hydrogen Energy* 40, 948–979. doi: 10.1016/j.ijhydene.2014.10.129
- Kraus, W., and Nolze, G. (2000). *POWDERCELL 2.4, Program for the Representation and Manipulation of Crystal Structures and Calculation of the Resulting X-ray Powder Patterns*. Berlin: Federal Institute for Materials Research and Testing.
- Krumm, S. (1996). An interactive windows program for profile fitting and size/strain analysis. *Mater. Sci. Forum* 228–231, 183–190. doi: 10.4028/www.scientific.net/MSF.228-231.183
- Künzner, N., Gross, E., Diener, J., Kovalev, D., Timoshenko, V. Y., and Wallacher, D. (2003). Capillary condensation monitored in birefringent porous silicon layers. *J. Appl. Phys.* 94, 4913–4917. doi: 10.1063/1.1609643
- Lehmann, V., Stengl, R., and Luigart, A. (2000). On the morphology and the electrochemical formation mechanism of mesoporous silicon. *Mater. Sci. Eng. B* 69–70, 11–22. doi: 10.1016/S0921-5107(99)00286-X
- Li, J., and Yoshizawa, K. (2015). Mechanistic aspects in the direct synthesis of hydrogen peroxide on PdAu catalyst from first principles. *Catal. Today* 248, 142–148. doi: 10.1016/j.cattod.2014.04.009
- Litovchenko, V. G., Gorbanyuk, T. I., and Solntsev, V. S. (2017). Mechanism of adsorption-catalytic activity at the nanostructured surface of silicon doped with clusters of transition metals and their oxides. *Ukr. J. Phys.* 62, 605–614. doi: 10.15407/ujpe62.07.0605
- Maity, S., and Eswaramoorthy, M. (2016). Ni-Pd bimetallic catalysts for the direct synthesis of H₂O₂ - unusual enhancement of Pd activity in the presence of Ni. *J. Mater. Chem. A* 4, 3233–3237. doi: 10.1039/C6TA00486E
- Melada, S., Rioda, R., Menegazzo, F., Pinna, F., and Strukul, G. (2006). Direct synthesis of hydrogen peroxide on zirconia-supported catalysts under mild conditions. *J. Catal.* 239, 422–430. doi: 10.1016/j.jcat.2006.02.014
- Menegazzo, F., Manzoli, M., Signoretto, M., Pinna, F., and Strukul, G. (2015). H₂O₂ direct synthesis under mild conditions on Pd–Au samples: effect of the morphology and of the composition of the metallic phase. *Catal. Today* 248, 18–27. doi: 10.1016/j.cattod.2014.01.015
- Munnik, P., de Jongh, P. E., and de Jong, K. P. (2015). Recent developments in the synthesis of supported catalysts. *Chem. Rev.* 115, 6687–6718. doi: 10.1021/cr500486u
- Ntainjua, E. N., Piccinini, M., Freakley, S. J., Pritchard, J. C., Edwards, J. K., Carley, A. F., et al. (2012). Direct synthesis of hydrogen peroxide using Au-Pd-exchanged and supported heteropolyacid catalysts at ambient temperature using water as solvent. *Green Chem.* 14, 170–181. doi: 10.1039/C1GC15863E
- Ogata, Y. H., Tsuboi, T., Sakka, T., and Naito, S. (2000). Oxidation of porous silicon in dry and wet environments under mild temperature conditions. *J. Porous Mater.* 7, 63–66. doi: 10.1023/A:1009694608199
- Ouyang, L., Tian, P.-F., Da, G.-J., Xu, X.-C., Ao, C., Chen, T.-Y., et al. (2015). The origin of active sites for direct synthesis of H₂O₂ on

- Pd/TiO₂ catalysts: interfaces of Pd and PdO domains. *J. Catal.* 321, 70–80. doi: 10.1016/j.jcat.2014.10.003
- Plyusnin, P. E., Baidina, I. A., Shubin, Y. V., and Korenev, S. V. (2007). Synthesis, crystal structure, and thermal properties of [Pd(NH₃)₄][AuCl₄]₂. *Russ. J. Inorg. Chem.* 52, 371–377. doi: 10.1134/S0036023607030138
- Polisski, S., Goller, B., Lapkin, A., Fairclough, S., and Kovalev, D. (2008). Synthesis and catalytic activity of hybrid metal/silicon nanocomposites. *Phys. Stat. Sol. B*, 132–134. doi: 10.1002/pssr.200802076
- Polisski, S., Goller, B., Wilson, K., Kovalev, D., Zaikovskii, V., and Lapkin, A. (2010). *In situ* synthesis and catalytic activity in CO oxidation of metal nanoparticles supported on porous nanocrystalline silicon. *J. Catal.* 271, 59–66. doi: 10.1016/j.jcat.2010.02.002
- Potemkin, D. I., Filatov, E. Y., Zadesenets, A. V., and Sobyanyin, V. A. (2017). CO preferential oxidation on Pt_{0.5}Co_{0.5} and Pt-CoOx model catalysts: catalytic performance and operando XRD studies. *Catal. Commun.* 100, 232–236. doi: 10.1016/j.catcom.2017.07.008
- Potemkin, D. I., Filatov, E. Y., Zadesenets, A. V., Snytnikov, P. V., Shubin, Y. V., and Sobyanyin, V. A. (2012). Preferential CO oxidation over bimetallic Pt-Co catalysts prepared via double complex salt decomposition. *Chem. Eng. J.* 207–208, 683–689. doi: 10.1016/j.cej.2012.07.037
- Potemkin, D. I., Semitut, E. Y., Shubin, Y. V., Plyusnin, P. E., Snytnikov, P. V., Makotchenko, E. V., et al. (2014). Silica, alumina and ceria supported Au-Cu nanoparticles prepared via the decomposition of [Au(en)₂]₂[Cu(C₂O₄)₂]₃•8H₂O single-source precursor: synthesis, characterization and catalytic performance in CO PROX. *Catal. Today* 235, 103–111. doi: 10.1016/j.cattod.2014.04.026
- Powder Diffraction File (2009). *PDF-2/Release 2009*. International Centre for Diffraction Data.
- Samanta, C. (2008). Direct synthesis of hydrogen peroxide from hydrogen and oxygen: an overview of recent developments in the process. *Appl. Catal. A* 350, 133–149. doi: 10.1016/j.apcata.2008.07.043
- Seo, M.-G., Kim, H. J., Han, S. S., and Lee, K.-Y. (2017). Direct synthesis of hydrogen peroxide from hydrogen and oxygen using tailored Pd nanocatalysts: a review of recent findings. *Catal. Surv. Asia* 21, 1–12. doi: 10.1007/s10563-016-9221-y
- Serp, P., and Castillejos, E. (2010). Catalysis in carbon nanotubes *ChemCatChem* 2, 41–47. doi: 10.1002/cctc.200900283
- Shubin, Y., Plyusnin, P., and Sharafutdinov, M. (2012). *In situ* synchrotron study of Au-Pd nanoporous alloy formation by single-source precursor thermolysis. *Nanotechnology* 23:405302. doi: 10.1088/0957-4484/23/40/405302
- Simonov, A. N., Plyusnin, P. E., Shubin, Y. V., Kvon, R. I., Korenev, S. V., and Parmon, V. N. (2012). Hydrogen electrooxidation over palladium-gold alloy: effect of pretreatment in ethylene on catalytic activity and CO tolerance. *Electrochim. Acta* 76, 344–353. doi: 10.1016/j.electacta.2012.05.043
- Smolentseva, E., Kusema, B. T., Beloshapkin, S., Estrada, M., Vargas, E., Murzin, D. Y., et al. (2011). Selective oxidation of arabinose to arabinonic acid over Pd-Au catalysts supported on alumina and ceria. *Appl. Catal. A* 392, 69–79. doi: 10.1016/j.apcata.2010.10.021
- Srinivas, S., Dhingra, A., Im, H., and Gulari, E. (2004). A scalable silicon microreactor for preferential CO oxidation: performance comparison with a tubular packed-bed microreactor. *Appl. Catal. A Gen.* 274, 285–293. doi: 10.1016/j.apcata.2004.07.012
- Svintsitskiy, D. A., Chupakhin, A. P., Slavinskaya, E. M., Stonkus, O. A., Stadnichenko, A. I., Koscheev, S. V., et al. (2013). Study of cupric oxide nanopowders as efficient catalysts for low-temperature CO oxidation. *J. Mol. Catal. A* 368–369, 95–106. doi: 10.1016/j.molcata.2012.11.015
- Tian, P., Xu, X., Ao, C., Ding, D., Li, W., Si, R., et al. (2017). Direct and selective synthesis of hydrogen peroxide over palladium-tellurium catalysts at ambient pressure. *ChemSusChem* 10, 3342–3346. doi: 10.1002/cssc.201701238
- Ueckert, T., Lamber, R., Jaeger, N. I., and Schubert, U. (1997). Strong metal support interactions in a Ni/SiO₂ catalyst prepared via sol-gel synthesis. *Appl. Catal. A* 155, 75–85. doi: 10.1016/S0926-860X(96)00384-5
- Vedyagin, A. A., Gavrilov, M. S., Volodin, A. M., Stoyanovskii, V. O., Slavinskaya, E. M., Mishakov, I. V., et al. (2013). Catalytic purification of exhaust gases over Pd-Rh alloy catalysts. *Top. Catal.* 56, 1008–1014. doi: 10.1007/s11244-013-0064-8
- Vedyagin, A. A., Volodin, A. M., Stoyanovskii, V. O., Kenzhin, R. M., Slavinskaya, E. M., Mishakov, I. V., et al. (2014). Stabilization of active sites in alloyed Pd-Rh catalysts on γ -Al₂O₃ support. *Catal. Today* 238, 80–86. doi: 10.1016/j.cattod.2014.02.056
- Wagner, C. D., Riggs, W. M., Davis, L. E., Moulder, J. F., and Muilenberg, G. E. (2013). *Handbook of X-Ray Photoelectron Spectroscopy*. Eden Prairie, MN: Perkin-Elmer.
- Yan, Y., Miao, J., Yang, Z., Xiao, F., Yang, H., Liu, B., et al. (2015). Carbon nanotube catalysts: recent advances in synthesis, characterization and applications. *Chem. Soc. Rev.* 44, 3295–3346. doi: 10.1039/C4CS00492B
- Yashtulov, N. A., and Flid, V. R. (2013). Regularities of formic acid oxidation in the presence of porous silicon nanocomposites with palladium. *Russ. Chem. Bull.* 62, 1332–1337. doi: 10.1007/s11172-013-0188-9
- Yashtulov, N. A., Gavrin, S. S., Bondarenko, V. P., Kholostov, K. I., Revina, A. A., and Flid, V. R. (2011). Formation of nanocomposite platinum catalysts on porous silicon. *Russ. Chem. Bull.* 60:434. doi: 10.1007/s11172-011-0068-0
- Yashtulov, N. A., Zenchenko, V. O., Kuleshov, N. V., and Flid, V. R. (2016). Synthesis and catalytic activity of platinum/porous silicon nanocomposites. *Russ. Chem. Bull.* 65, 2369–2374. doi: 10.1007/s11172-016-1591-9
- Yi, Y., Wang, L., Li, G., and Guo, H. (2016). A review on research progress in the direct synthesis of hydrogen peroxide from hydrogen and oxygen: noble-metal catalytic method, fuel-cell method and plasma method. *Catal. Sci. Technol.* 6, 1593–1610. doi: 10.1039/C5CY01567G
- Zhai, W., Ai, Q., Chen, L. N., Wei, S. Y., Li, D. P., Zhang, L., et al. (2017). Walnut-inspired micro-sized porous silicon/graphene core-shell composites for high-performance lithium-ion battery anodes. *Nano Res.* 10, 4274–4283. doi: 10.1007/s12274-017-1584-5
- Zhao, M., Yuan, K., Wang, Y., Li, G., Guo, J., Gu, L., et al. (2016). Metal-organic frameworks as selectivity regulators for hydrogenation reactions. *Nature* 539, 76–80. doi: 10.1038/nature19763

Conflict of Interest Statement: The authors declare that the research was conducted in the absence of any commercial or financial relationships that could be construed as a potential conflict of interest.

The reviewer, YZ, and handling Editor declared their shared affiliation.

Copyright © 2018 Potemkin, Maslov, Loponov, Snytnikov, Shubin, Plyusnin, Svintsitskiy, Sobyanyin and Lapkin. This is an open-access article distributed under the terms of the Creative Commons Attribution License (CC BY). The use, distribution or reproduction in other forums is permitted, provided the original author(s) and the copyright owner are credited and that the original publication in this journal is cited, in accordance with accepted academic practice. No use, distribution or reproduction is permitted which does not comply with these terms.